

## Skin Derived Stem Cells Scaffold Regenerate Axons of Injured Dorsal Root

F. Colleoni<sup>1</sup>, M. Pluder<sup>2</sup>, M. Belicchi<sup>1</sup>, P. Razini<sup>1</sup>, N. Bresolin<sup>3</sup>, D. Spagnoli<sup>4</sup>, F. Raneri<sup>2</sup>, P. Rampini<sup>2</sup>, S. Gatti<sup>2</sup>, M. Vergari<sup>5</sup>, N. Grimoldi<sup>2</sup>, Y. Torrente<sup>1</sup>

<sup>1</sup>Stem Cell Laboratory, Department of Pathophysiology and Transplantation, Università degli Studi di Milano, Fondazione IRCCS Ca' Granda Ospedale Maggiore Policlinico, Milan, Centro Dino Ferrari, Milan, Italy

<sup>2</sup>Neurosurgery Unit, Fondazione IRCCS Ca' Granda Ospedale Maggiore Policlinico, Università degli Studi di Milano, Milan, Italy

<sup>3</sup>Neurology Unit, Department of Pathophysiology and Transplantation, Università degli Studi di Milano, Fondazione IRCCS Ca' Granda Ospedale Maggiore Policlinico, Milan, Centro Dino Ferrari, Milan, Italy

<sup>4</sup>Neurosurgery Unit, Ospedale Moriggia Pelascini, Gravedona, Italy

<sup>5</sup>Neurophysiopathology Unit, Fondazione IRCCS Cà Granda Ospedale Maggiore Policlinico, Milan, Italy

*Corresponding Author:* Yvan Torrente, MD; e-mail: yvan.torrente@unimi.it;  
Nadia Grimoldi, MD; e-mail: nadia.grimoldi@unimi.it

**Keywords:** Skin derived stem cells, Spinal root regeneration, Scaffold.

### ABSTRACT

**Introduction:** Lesion to the dorsal spinal roots can prove to be severely debilitating, with poor prognoses leading to a permanent loss of sensory information.

**Background:** The transplantation of several cell types, especially embedded in a supporting scaffold, was demonstrated to be effective in enhancing regeneration response. In our previous study we described the properties of Skin Derived Stem Cells (SDSCs) to differentiate in glial elements and contribute to peripheral nerve regeneration.

**AIM:** In this study we evaluated the effect of SDSCs in the regeneration of spinal root injury.

**Materials and Methods:** We mechanically eradicated rat IV somatosensory lumbar root to generate injury, reposed it keeping it in position by using a vicryl scaffold, seeded with SDSCs and evaluated their efficacy through in vivo cell imaging, histological and electrophysiological analysis.

**Results:** We showed that SDSCs seeded on vicryl scaffold could be maintained at the peripheral and CNS interface facilitating axonal regrowth. After DR section, we observed restored anatomical continuity, axonal regrowth and partial recovery of the somatosensory defect.

**Discussion:** This study demonstrates the efficacy of SDCSc transplanted in supporting the regeneration of the injured DR. Combining it with scaffolding allows to maintain the avulsed root in the

**right position. This study confirms the usefulness of SDSCs in supporting regeneration of DR axons and proposes these cells as a possible therapeutic tool in CNS injury.**

**Conclusion:** This combination treatment provides cues to the improvement of recovery after dorsal root injury.

### INTRODUCTION

Brachial plexus injury is a serious medical problem that annually affects many patients. Approximately 60-70% of these injuries involve root damage or avulsion<sup>1</sup>, and although many of these roots can be surgically reimplanted, functional recovery in the affected limb is rarely achieved<sup>2</sup>, due to a limited or null axons regeneration across excision gaps larger than 4 mm. Furthermore, the regeneration of injured central axons of Dorsal Root Ganglion (DRG) neurons, abruptly stops at the interface between the central (CNS) and the peripheral nervous systems, a domain called the dorsal root entry zone (DREZ), with permanent somatosensory defects<sup>3,4</sup>. Successful experimental interventions, used to promote regeneration of axotomized axons, have relied on blockade of inhibitory cues, involving the glial scar in the injury site<sup>5-10</sup>; supplementation of growth-promoting cues such as neurotrophic factors, extracellular matrix components or biopolymers<sup>11-17</sup>; cellular transplantation<sup>8,18-21</sup> and stimulation with agents capable of facilitating or activating neuronal regeneration<sup>22-24,26</sup>. Whereas treatments targeting these processes have individually proven efficacious in fa-

cilitating regeneration and functional recovery, the number of regenerating axons is generally small, illustrating the need to overcome multiple factors that limit axon growth. It is therefore necessary to develop therapeutic methods that can help these regenerating root pathways to overcome the inhibitory signals. The combination of stem cell grafting with scaffold support has been recently developed for nerve repair and plays an important role in nerve growth and guidance. Neural Stem Cells (NSCs) can differentiate into supportive cells and contribute to promotion of axonal regeneration<sup>27</sup>. However, the use of autologous NSCs has several clinical limitations, including a readily, accessible source of these cells<sup>28,29</sup>. Skin Derived Stem Cells (SDSCs) are able to regenerate nerves with nerve guides<sup>30</sup>, whereas bone marrow mesenchymal stem cells, *in vitro*, are able to express glial markers and induce nerve regeneration with glial growth<sup>31-35</sup>. We therefore assumed that the combination of autologous SDSCs as accessible sources of stem cells for nerve regeneration and a scaffold aimed at restoring anatomical continuity after DR section or avulsion, would improve functional outcome after brachial plexus injury. In this study, we investigate an implantable vicryl scaffold, seeded with SDSCs, that provides signals for cell attachment and growth as a potential treatment for nerve root avulsion.

## MATERIALS AND METHODS

### CELL CULTURE

Cells were isolated from two-day-old new born Wistar rats, as described in our previous works<sup>36,37</sup>. Skin tissues were dissected and minced into smaller pieces using sharp razors. Specimens were washed with EBSS and enzymatically dissociated adding 0.2% collagenase type XI and 0.1% trypsin for 1 h at 37°C. The cell extract was filtered with a 70 µm nylon mesh (DAKO) and subsequently plated on non coated flasks to offer the advantage of isolating different populations of skin-derived cells. Preplate 1 (pp1) represented a population of skin-derived cells that adhered in the first 24 hours after isolation and highly enriched with fibroblasts. Preplate 2 (pp2), represented a population of skin-derived cells that did not adhere, was used as the target population. The growth media was composed of Dulbecco's Modified Eagle Medium: Nutrient Mixture F-12 (DMEM/F-12, 1:1), 20% Fetal Bovine Serum (FBS), including HEPES buffer (5 mM), glucose (0.6%), sodium bicarbonate (3 mM), and glutamine (2 mM). Hormone and salt

mixture composed of insulin (25 µg/mL), transferrin (100 µg/mL), progesterone (20 nM), putrescine (60 µM), and sodium selenite (30 nM) was also used. Mitogens, epidermal growth factor (EGF) (20 ng/mL) and fibroblast growth factor (bFGF) (10 ng/mL) (murine recombinant; Chiron Corporation, Emeryville, CA) were added to the above medium.

### SELF-MAINTENANCE AND *IN VITRO* DIFFERENTIATION OF SDSCs

Self-maintenance of skin-derived progenitors was tested as previously described<sup>30</sup>. Briefly, the pp2 floating spheres were mechanically dissociated and plated as a single cell after limiting dilution in a 96-well plate with a mitogen added medium and the secondary and tertiary sphere formations were evaluated. In differentiation experiments, the spheres were isolated and plated on glass coverslips and cultured in DMEM/F-12 medium with the hormone and salt mixture, EGF and bFGF. Coverslips were processed 21-25 days later for indirect immunofluorescence. They were fixed in 4% paraformaldehyde in 1X Phosphate Buffered Saline (PBS), pH 7.2, for 30 min, washed in PBS, pH 7.4, and after incubation in blocking solution, incubated with primary antibodies (Glial Fibrillary Acidic Protein GFAP; Sigma, 1:300 and Nestin; BD Pharmingen, 1:50) for 90 mins. The cells were then incubated with appropriate secondary 488/594-conjugated IgG antibodies (Molecular probes, 1:100) for one hour at room temperature<sup>30</sup>. Nuclei were counterstained with 4',6-diamidin-2-fenilindolo (DAPI, Sigma). The slides were examined by fluorescence microscope LEICA DMIRE2 and images were acquired by LEICA Qfluoro software. SDSCs at pp2 passage were transduced with a lentiviral vector expressing the enhanced green fluorescent protein (eGFP).

10<sup>7</sup> to 10<sup>8</sup> ip/ml were used to transduce 10<sup>5</sup> cells. Vector transduction was performed in 500 µl of DMEM supplemented with 10% FCS. Four hours after transduction medium was diluted by adding 500 µl per well of previous medium. The dishes were incubated for 24 hr at 37°C and 5% CO<sub>2</sub> before washing. Engineered cells were then placed on Vicryl scaffold.

### VICRYL SCAFFOLD

Vicryl (polyglactin 910) is a synthetic, slowly absorbing surgical suture material made of copolymer of lactide and glycolide, available as a braided suture and manufactured by Ethicon Inc (Somerville, NJ, USA). Its purpose is the approximation and ligation of soft tissues. The Vicryl suture is completely

absorbed within 70 days. Vicryl may also be treated for more rapid breakdown in quick healing tissues, such as mucous membrane, or embedded in triclosan to provide antimicrobial protection of the suture line.

#### SURGICAL PROTOCOL

Forty-two Wistar rats (age: 2 months; weight: 170-200 grams) were submitted to the surgical protocol. All surgical procedures were performed respecting Italian Guide Lines concerning the use of laboratory animals. Surgery was carried out in aseptic conditions with the aid of a microscope. Anesthesia was induced by an intraperitoneal injection of Cloralum Hydrate (2 ml, 6.25%). A linear incision was made in the midline at a dorsal-lumbar level with the rodents in a prone position. The paravertebral muscles were retracted to expose the spinous processes and laminae of the lumbar vertebrae. A left hemilaminectomy of the upper two lumbar vertebrae was performed with a microdrill. After opening the dura the

thoracic spinal cord, the conus medullaris and the proximal roots of the cauda equina were exposed. At the level of the conus, the fourth lumbar root (L4) was anatomically identified, due to its larger diameter and its downwards direction (Figure 1 A,B). The somatosensory dorsal component of L4 was dissected and a 10-0 non re-absorbable thread was delicately tied around it in order to keep it well distinguishable during the procedure and after animal sacrifice. The dorsal rootlet was then carefully isolated and sectioned at its entry into the spinal cord at the height of the dorsal root entry zone (DREZ) and injected with the anterograde tracer (Figure 1 C,D). In 21 rats (control group) the sectioned rootlet was hence repositioned at its original entry site into the spinal cord and fixed with fibrin glue. In other 21 operated rats (experimental group) the sectioned dorsal root was placed in the original entry site on spinal cord through a vicryl scaffold

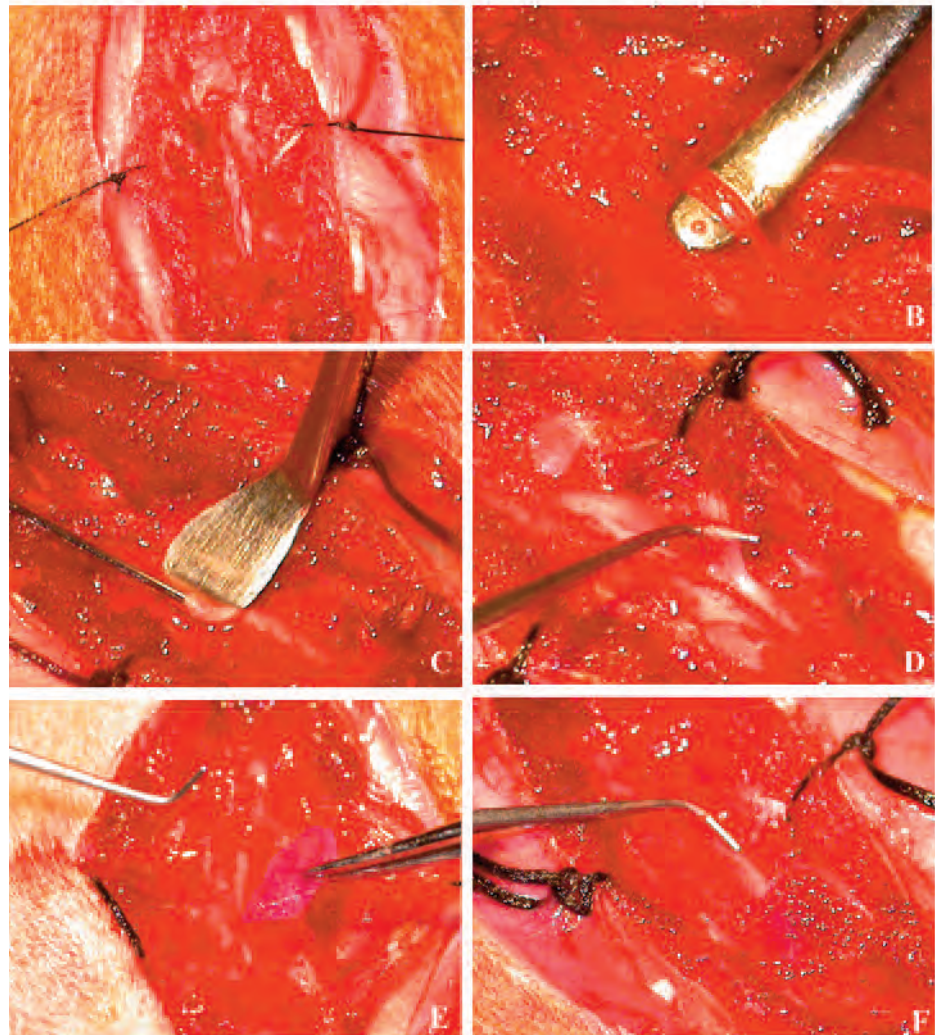


**Figure 1.** Surgical procedures of dorsal root injury. The thoracic spinal cord, the conus medullaris and the cauda equina were exposed after an hemilaminectomy of the upper two lumbar vertebrae and the opening of the dura (A). The fourth somatosensory lumbar root was identified (B). It was sectioned and injected with Cholera Toxin subunit B (C). Immediately after the injection, the root was reposed in proximity of the spinal cord, at the DREZ (D). The SDSCs embedded Vicryl (E) was wrapped around the avulsed root reposed in contiguity with spinal cord at the level of the DREZ (F).

embedded with GFP-labelled cultured SDSCs (Figure 1E, F). All animals were sacrificed, at 7 (n=7 per each group), 30 (n=7 per each group) and 90 days (n=7 per each group). Before reconnection, the sectioned DRs were slowly injected with the Alexa Fluor<sup>®</sup> 488 cholera toxin subunit B (Molecular Probes) for *in vivo* intravital microscopy and with Alexa Fluor<sup>®</sup> 594 cholera toxin subunit B for tissue analysis. The use of the two different dyes was due to the technical limitation of *in vivo* imaging as described in the relative section.

#### SDSCs AND SCAFFOLD IMPLANT AT THE SITE OF THE LESIONED DREZ

10<sup>6</sup> GFP expressing SDSCs were seeded in a small bundle of Vicryl fibers (total volume: 1-2 mm<sup>3</sup>) for 3 days at 37° C. These offered a support for the implanted SDSCs, avoided their dispersion into surrounding structures and contributed to keeping them in place. Both the scaffold and the stem cells wrapped around the rootlet had been repositioned at the DREZ and fixed with fibrin glue.

#### ELECTROPHYSIOLOGICAL STUDY: MEASUREMENT OF CORTICAL SENSORY EVOKED POTENTIALS

Cortical Sensory Evoked Potentials (SEPs) were recorded from a needle electrode inserted subcutaneously over the hind limb projection area of the somatosensory cortex. The active electrode was placed 9 mm anterior and 2 mm lateral to the bregma. A reference electrode was placed 20 mm anterior to the bregma at the midline and a ground electrode was attached to the animal's tail. SEPs were recorded using a Micromed Myohandy-1200 EMG/EP measuring system, with a filter set to bandwidth 20-3000 Hz. The contralateral femoral nerve was stimulated distally at the anterolateral aspect of the thigh with a bipolar electrode anode. Stimuli duration was 0.2 ms, repetition rate was 3 Hz, and intensity was 10 mA, sufficient to produce a definite twitch of the big toe. For each set of recordings the average of 200 responses was taken and the recordings were done twice to ensure response reproducibility. Hind limb transcutaneous stimulation evoked electrical activity with prominent first-positive (P1), first-negative (N1) and second-positive (P2) components. A negative wave was expressed as an upward deflection. We measured peak latency and peak-to-peak amplitude for each component in order to quantify neuronal responses to somatosensory stimulation. SEPs were recorded

before surgery, after one and three months from surgical procedure, in both cell implanted and control animal groups.

#### IMMUNOFLUORESCENCE ANALYSIS

Immunofluorescent stainings of tissue were done at different points: 7, 30, and 90 days after surgery. Spinal cords were removed, fixed in 4% paraformaldehyde for 2 hours, dehydrated in 30% sucrose over night, frozen in liquid nitrogen-cooled isopentane and stored at -80°C until sectioning. Both longitudinal and transverse sections of 10 µm thickness were cut on a cryostat. Sections were fixed in 4% paraformaldehyde for 4 min, incubated in blocking solution for 30 mins and with primary antibodies anti-laminin (Sigma, 1:50) and anti-neurofilament-180 (Chemicon 1:50) incubated with respective secondary antibodies (Alexa Fluor 488 conjugated anti-rabbit IgG, 1:100, Molecular Probes). Grafted cells were detected by immunofluorescence assays for GFP-positive cells with polyclonal anti-GFP 488 (1:50 Molecular Probes). Cell nuclei were stained with DAPI. Slides were analyzed by Leica TCS-SP2 confocal microscope.

#### INTRAVITAL MICROSCOPY

Intravital microscopy was assessed by Cellvizio<sup>®</sup> (Mauna Kea Technologies, Paris, France 39) configured for 488 nm wavelength excitation, optimal for GFP detection. Due to the limited excitation, for this specific experiment, we used the 488 conjugated version of the CTB tracer. GFP<sup>+</sup>-SDSCs and the fluorescent green tracer were visualized seven days after grafting (n=7 per control and experimental group). Anesthetized rats were positioned on a stereotaxic apparatus. A window was made on the rodents' backs, in correspondence to the lesioned root to allow penetration of a ProFlex fiber optic, connected to an endoscope probe (S1500). The Proflex endoscope probe was handled by stereotaxic apparatus.

## RESULTS

### ISOLATION AND CHARACTERIZATION OF SDSCs

The rat SDSCs by 3-7 days from dissociation grew as floating clusters of cells with morphological resemblance to spheres. At cytofluorimetric analysis, they were lineage negative (CD33<sup>-</sup>, CD38<sup>-</sup>, CD45<sup>-</sup>, CD34<sup>-</sup>, express Thy1<sup>+</sup>/CD90 (30%) and possessed clonal capacity as previously described<sup>(30, 36)</sup>. To evaluate the proportion of neural progenitors in the cultures, spheres were disaggregated into single cells that were plated, fixed, and ana-

lyzed for the expression of the early neural marker (Figure 2 C-F). A high proportion of the cells expressed nestin ( $80 \pm 1.6\%$ ,  $n = 10$  experiments) and vimentin ( $80.5 \pm 1.5\%$ ,  $n = 6$ ). These proportions were stable during cultivation of the spheres (up to 12 weeks). After plating on laminin-coated dishes in a B27 neurobasal medium supplemented with serum, skin-derived spheres generated cells positive for the astroglial marker GFAP ( $75 \pm 3.1\%$ ,  $n = 10$  experiments) (Figure 2 A,B). Oligodendrocyte lineage cells were infrequent under our culture conditions and few cells were immunoreactive to O4, an antibody recognizing oligodendrocyte-specific glycolipids (data not shown). Single-cell-derived primary SDSCs spheres generated clonally derived secondary spheres capable of producing, after their dissociation, tertiary spheres which could be differentiated into cells expressing prevalently astroglial markers. All these data demonstrated the stem cell characteristics of the SDSCs. The rat SDSCs were transfected with GFP and analyzed by citofluorimetric analysis after 24 hours. The mean transfection efficiency, was lower than expected assessing at  $40 \pm 2.8\%$  ( $n = 10$  experiments) due to the property of these cells to grow in very dense spheres. These spheres could not be completely dissociated without inducing physical stress to the cells and, as a consequence of this poor dissociation, the cells constituting the inner part of the spheres were barely transfected with good efficiency.

#### SDSCs ADHESION ON VICRYL SCAFFOLD

GFP<sup>+</sup>-SDSCs were seeded and cultured on a sterilized Vicryl scaffold for at least seven days. During this period the cells were viable and maintained the GFP protein, expressed even if in a low percentage. The scaffold is constituted by polyglycolic acid filaments which tangle up randomly when put in medium filled wells. Vicryl is a congenial material for the cells, that tend to lay down on the filaments, growing in big cluster wrapped around the fibers while only a few adhered to the bottom of the plate or remained floating in the medium (see Figure 2 C and D).

#### GROSS FINDINGS REVEALED NO SIDE EFFECTS OF SURGICAL SDSCs TRANSPLANTATION

Dorsal root injury was carried out by a specific surgical procedure as described in the Method section. Briefly, after the retraction of the paravertebrale muscles, a left emilaminectomy of the first lumbar vertebra was performed, the dura was opened and the distal spinal cord with cauda equina roots were exposed. Forty-two treated rats were sacrificed at 7 ( $n=7$  per each group), 30 ( $n=7$  per each group) and 90 days ( $n=7$  per each group). At sacrifice, only animals with the nerve root stump correctly juxtaposed to the spinal cord DREZ were considered. Neither septic collections nor tumorigenesis were observed at the site of nerve lesion. Fibrin glue in-

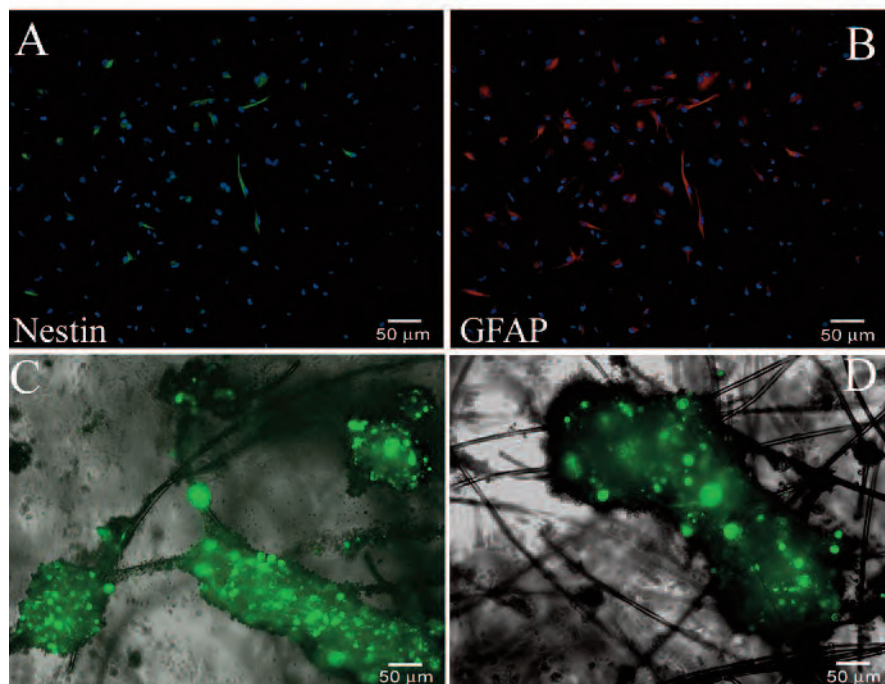


**Figure 2.** *In vitro* properties of SDSCs. Under differentiating conditions, these cells maintain the neural stemness marker nestin (A-green) and express the glial marker GFAP (B-red). Following GFP transfection, SDSCs grow on the Vicryl scaffold adhering around the filaments in big clusters (C, D). Bars labelled with measurements in each panel.

jected during the surgical procedure had been completely reabsorbed. Nervous tissue contusions or hyperhaemia were not observed in the spinal cord of treated rats. Control animals, treated with vicryl scaffold, not seeded with SDSCs, showed the rootlet fixed to the DREZ by a thin fibrous reaction without a thorough integration to the spinal cord. On the other hand, the animals which were treated with vicryl scaffold, seeded with SDSCs, showed sectioned sensory rootlets correctly connected through the DREZ to the spinal cord. In all 42 treated animals, no cases of postsurgical spinal cord

lesions were observed. Moreover, no signs of autotomy were recorded one and three months after treatment with vicryl scaffold seeded with SDSCs, demonstrating the absence of dysesthesia or hyperpathia (Figure 3 A).

#### RESCUE OF DR INJURY WITH VICRYL SCAFFOLD SEEDED WITH SDSCs

Repositioning after wrench of the DR, enveloped with the vicryl scaffold, should exert the effect of reconstituting direct physical contact between the Schwann cells of the avulsed root, activated by the injury, and the astrocytes at the entry point on the spinal cord. The reconnection of sectioned DR was

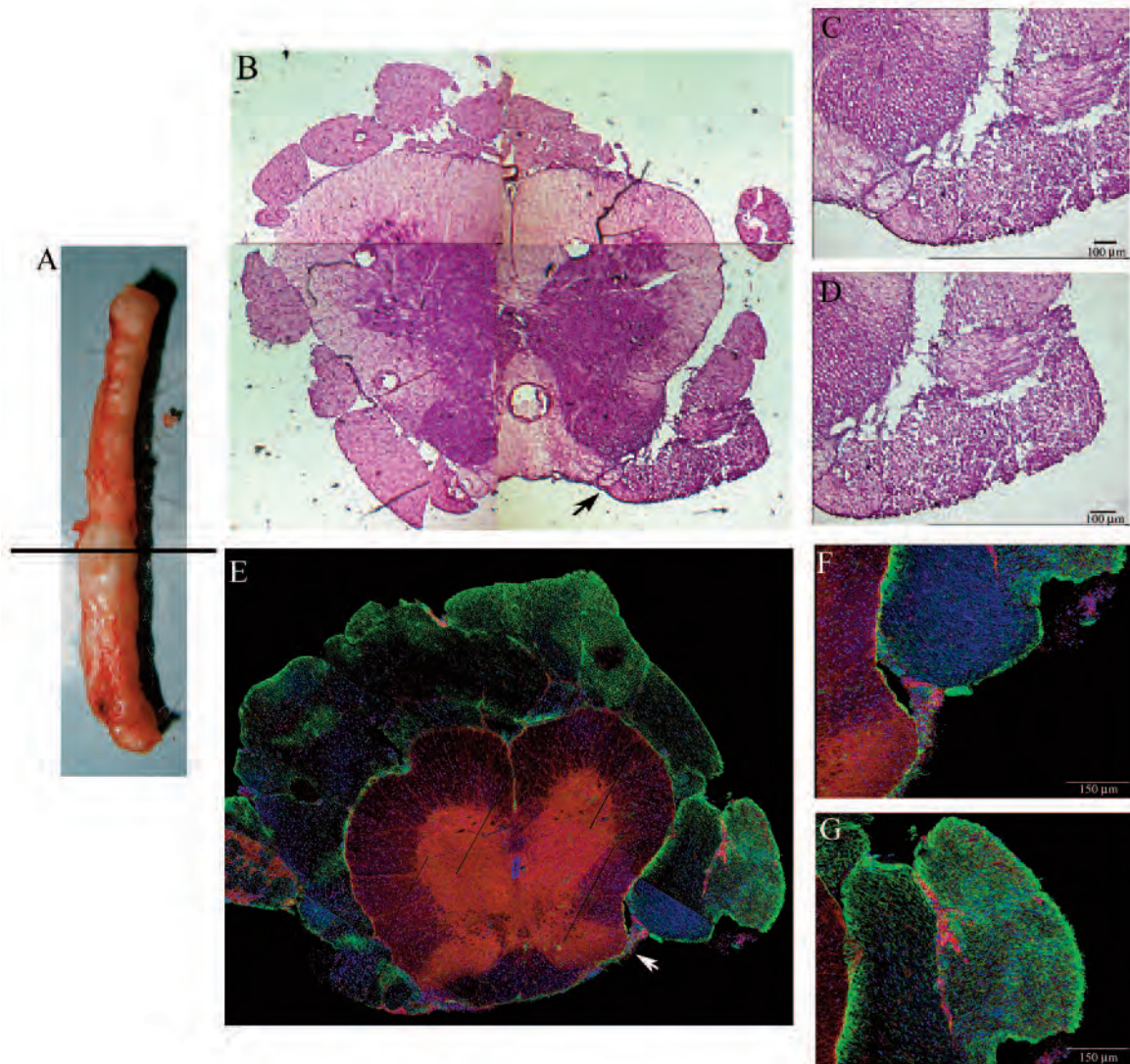


**Figure 3.** We analyzed histological aspects of the spinal cord 1 and 3 months after transplantation. *A*, spinal cord as it appears at sacrifice; black line indicates the lesion site analyzed in further histological images. *B*, haematoxylin & eosin staining of the whole spinal cord section evidences the presence of the spinal roots, maintained in the right anatomical position (arrows). *C* and *D*, detailed images of the transition zone between the spinal cord and the root: the root shows no sign of inflammation and are well connected with the spinal cord. *E*, Immunofluorescence analysis detecting the CTB-Alexa Fluor®594 (red) enter from the root. *F-G*, detailed images demonstrate tracer (red) transition from laminin positive root (green), into the spinal cord. Bars labelled with measurements in each panel.

demonstrated by histological and immunofluorescence analysis of transversal sections at one and three months after SDSCs grafting. The H&E analysis demonstrate the correct repositioning of sectioned DR in the spinal cord (see Figure 3 B, C and D). The cholera toxin subunit B is a transganglionic marker which, when injected in the periphery, is retrogradely transported to DRG neurons and then anterogradely transported from DRG neurons to the spinal cord. CTB tracer was applied to the sectioned DRs before their reconnection. Fluorescence staining of the spinal cord was examined one week later. In control rats, CTB tracer fluorescent signal was not detected in the spinal cord. The spinal cords of rats treated with vicryl scaffolds, seeded with SDSCs, were labelled with CTB tracer and essentially detected in deep laminae III-X and in deeper laminae of the spinal

cord dorsal horn (see Figure 3 E, F and G). Confocal microscopy analysis indicated that a fraction (estimated in the range of 50%) of the fibers labelled, with CTB tracer, were stained with anti-NF180 and anti-laminin antibody (Figure 4). Because the lumbar DRs had been sectioned in these rats before tracer injection, these results demonstrated that the DRG neurons projected central axons into the spinal cord dorsal horn through the vicryl scaffold, seeded with SDSCs. Several GFP expressing SDSCs were found around reconnected DR and in the DREZ (data not shown). Furthermore, we could visualize several tracer positive neuron bodies in the contralateral and anterior spinal cord area, indicating the active connection with interneurons (see Figure 4).

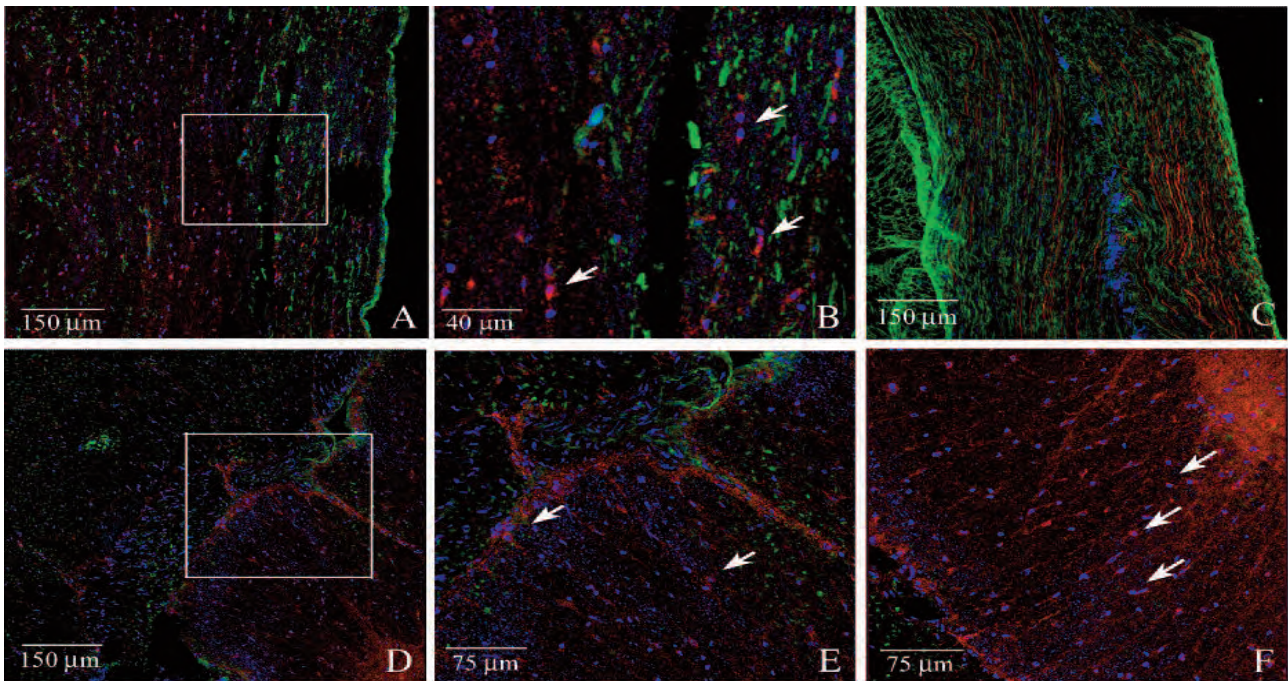
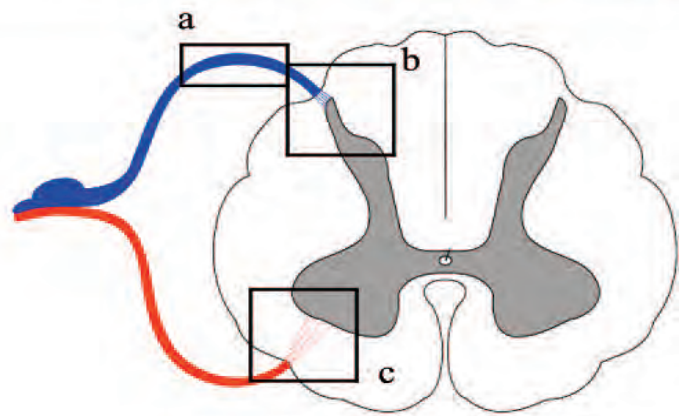


**Figure 4.** Reconnection between avulsed root and spinal cord. Boxes on the spinal cord layout, visualize the areas detailed in the figures. We focused on the DREZ area (a), posterior (b) and anterior (c) horns. Longitudinal sections of DREZ (a) stained with CTB Alexa Fluor 594 (red) and NF180 (green - A and higher magnification in B) and laminin (green - C) show the presence of the tracer through the root. Transversal images of b and c areas: CTB (red) and Nf180 (green) in D (higher magnification in E) and F demonstrate the presence of the tracer within the spinal cord. Arrows label double positive axons of the root (E) and CTB positive neuron bodies in the spinal cord (E-F). Bars labelled with measurements in each panel.



Further substance, in demonstrating the presence of GFP-expressing SDSCs in the lesion site, was offered by intravital microscope Cellvizio®. This microscope allows the *in vivo* visualization of fluorescent trackers/cells by different sized probes. Before sacrifice, the animals were anesthetized and the reconnected DRs were exposed; by the positioning of the S1500 probe along the damaged area, we were able to visualize several GFP<sup>+</sup>-SDSCs localized around the reconnected DRs. This finding highlighted the role of the Vicryl scaffold in avoiding cells spreading that could optimize the transplant efficiency. Numbers of GFP<sup>+</sup>-SDSCs were visualized after the reconnection assessed at  $5 \pm 2$  per field (Figure 5 A, B). In addition, we used intravital microscopy to follow the fate of CTB-Alexa Fluor® 488 tracer after injection. This technique enabled the visualization of the ascending course of

the tracers from the root towards the spinal cord detecting the single 488-positive fibers after the functional reconnection between root and spinal cord (Figure 5 D-F).

#### ELECTROPHYSIOLOGICAL EVALUATIONS SHOWED REPAIRED SENSORY PATHWAYS IN ANIMALS TREATED WITH VICRYL SCAFFOLD SEEDED WITH SDSCS

Cortical SEPs were recorded over the hind limb projection area of the somatosensory cortex by distal stimulation of contralateral femoral nerve. Latencies and peak-to-peak amplitudes were recorded in all animals before surgery (baseline), at one month and at three months after surgical procedure. The electrophysiological recovery resulted higher in the animals implanted with SDSCs and the scaffold. In both groups of animals we observed a reduction in amplitude of the recorded cortical SEPs. The amplitudes reached 70% of the baseline SEPs in the stem cell implanted group at one month and 80% of

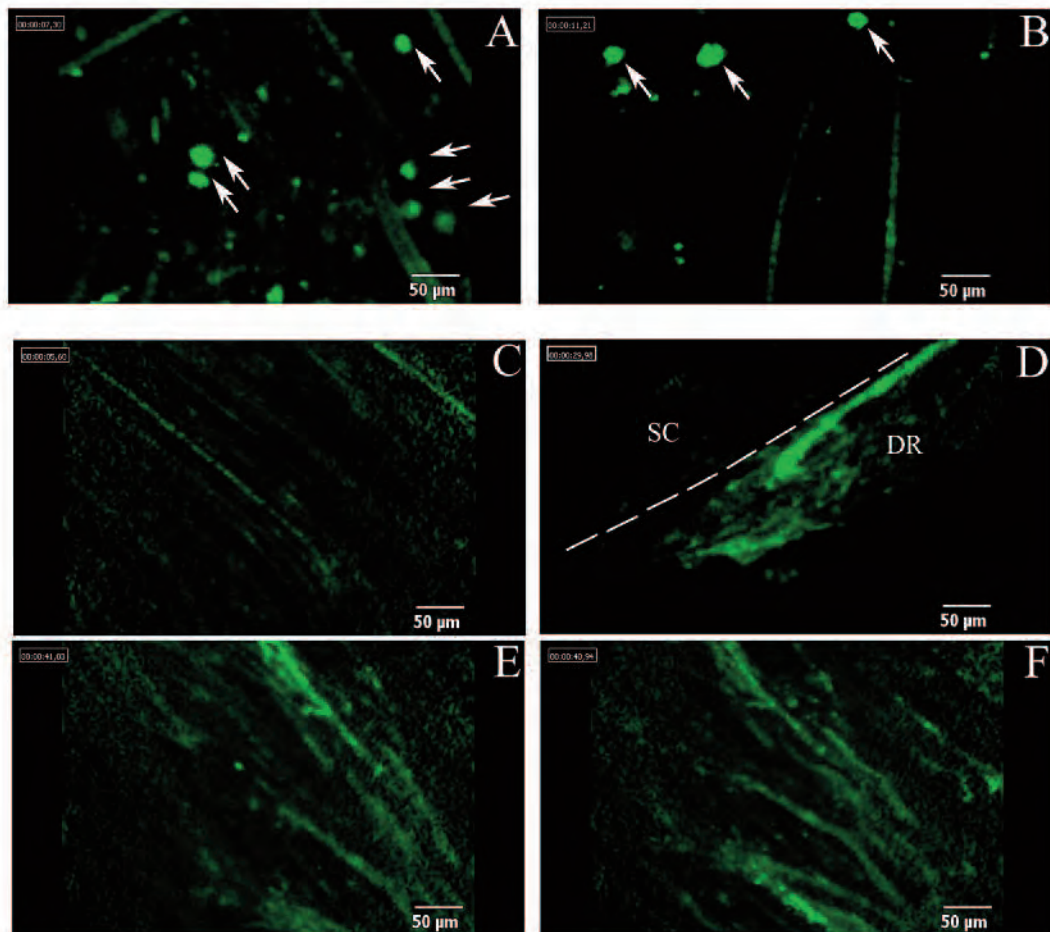


**Figure 5.** A-B, GFP<sup>+</sup>-SDSCs cells observed by intravital microscopy. Near the DREZ we could visualize green round shaped cells in different fields of treated animals. C, Avulsed, but non-reposed root, shown as negative control. D, E and F, pathway of the CTB-Alexa Fluor®488 through the dorsal root (DR) proximal tract, upstream to the lesion, and the positive fibres in the first tract of spinal cord (SC). Bars labelled with measurements in each panel.



the baseline at three months after the surgical procedure. In the control group, peak amplitudes remained 50% of baseline amplitudes at one month and at three months after surgery. Latencies showed a mean increase of 27% at N1 peak and of 31% at P1 peak at three months in the cell implanted group in comparison to the baseline, while the control group showed an average of a 50% increase of the baseline values (Figure 6).

## DISCUSSION

Among nervous system lesions, DR injuries are often neglected because most research attention often focuses on the more frequent spinal cord or peripheral nerves injuries. Presently, the treatment for brachial plexus injuries resides on a surgical procedure to restore shoulder and elbow movements, but with respect to sensory repair current surgical approaches are often disappointing.

This study aimed to find a new combined strategy to improve the therapeutic approach in restoring sensory pathways involved in these lesions.

In nervous system lesions, several cell types were used to enhance regenerating response.

Embryonic stem cells and induced pluripotent stem cells have been investigated in their safety and efficacy in SCI models<sup>39-41</sup>; neural stem/progenitor cell transplants are widely used, as they are able to generate glial cells *in vivo*<sup>42</sup>, not always successfully however<sup>43</sup>; olfactory ensheathing cells are a special class of glial cells often used in neural tissue regeneration<sup>43,44</sup>, and have been reported as electrophysiological evidence of the recovery of motor-evoked potentials and axonal regeneration after OEC injection into a complete transection lesion<sup>45</sup>; Schwann cells, after transplantation, express various numbers of adhesion molecules and contribute to remyelina-

tion<sup>46</sup>; mesenchymal stem cells, derived from bone marrow or other different tissues after implant in spinal cord injury, often do not differentiate in neuronal cells<sup>47-49</sup> but create a favorable environment for functional recovery, secreting neurotrophic factors and modulating inflammation after injury<sup>47,48,50,51</sup>.

Our background on stem cells research led us to isolate a multipotent stem cell population, derived from the dermis: the SDSCs. These cells are able to generate neural lineage cells *in vitro* and *in vivo*<sup>36,52,53</sup> and when transplanted into a sciatic nerve regeneration model, they showed a good survival rate and efficacy in producing a favorable environment for the regenerating axons, mainly improving vascularization<sup>30</sup>. Furthermore, after preclinical safety studies, we grafted SDSCs in a compassionate case of nerve poly-injured patient which reported several upper arms damages. After 3 years of follow up we observed a slight sensory and motor recovery and a maintained trophism of tissues, preventing arms amputation<sup>54</sup>.

These cells were then used as candidates for reproducing this healthy effect in our CNS lesion model. The model consists of a mechanical eradication of rat IV somatosensory dorsal root to generate injury and a repositioning in the lesion site of the avulsed root embedded in a vicryl scaffold and seeded with autologous SDSCs.

For an optimal functional recovery, the avulsed axons needed to be directed and guided through the lesion gap and supported in restoring the synaptic signal in the spinal cord. Furthermore, the transplantation of cell suspension, directly into the spinal cord without scaffold, is not useful because it could

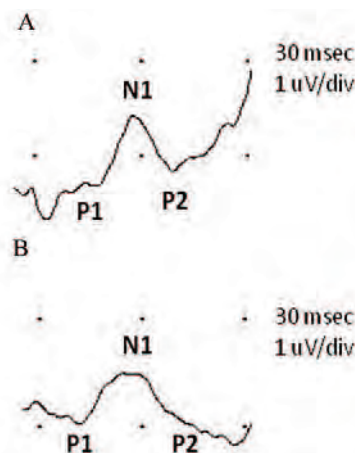


**Figure 6.** Cortical SEPs recorded over the hind limb projection area of the somatosensory cortex by distal stimulation of contralateral femoral nerve. A, latencies and peak-to-peak amplitudes recorded before surgery (baseline). B, electrophysiological recovery at one month after surgical procedure, in the animals implanted with SDSCs. The amplitudes reached 70% of the baseline SEPs.

Baseline	P1	N1	P2
Latency (msec)	15,93	19,35	22,95
Amplitude peak-peak (uV)	1,47	1,17	

Post 4 weeks	P1	N1	P2
Latency (msec)	13,98	19,23	24,17
Amplitude peak-peak (uV)	0,98	0,88	

not provide a continuous bridge of cells from the injured root to the DREZ<sup>55,56</sup>. For these reasons, to enhance regeneration of DRG sensory axons and to keep the transplanted cells in loco, we applied a Vicryl scaffold embedded with the cells around the lesioned root and between the two edges. Our scaffold has been widely used as suture, therefore showing a high biocompatibility and rapid absorption. Furthermore, SDSCs, cultured on Vicryl filaments, showed a high affinity for the material, they adhered and grew in spheres enveloping the filament, allowing for easy positioning in the lesion site.

After one and three months post-surgery, we did not observe any scaffold residual, with absent fibrotic reaction, suggesting non-immunogenic response to the transplanted cells. Morphological analysis provided evidence for an anatomical connection between the sectioned DR and spinal cord, through vicryl scaffold, seeded with SDSCs.

The presence of some vital cells at the transplantation site, as demonstrated by intravital microscopy, means that the environment is still permissive to their survival, probably due to the contribution of factors secreted by the cells themselves.

In the end, finding the live cells at the lesion and anatomical continuity between the two lesioned stumps, is not necessary meaningful of functional reconnection between the two lesions' borders.

To detect this reconnection, and the effective transmission of some signals through the lesioned root, we injected tracer cholera toxin subunit B (CTB) into intact nerves, which preferentially stains medium and large diameter myelinated primary afferent axons, as visualized in the case of reconnected DR with vicryl scaffold seeded with SDSCs. CTB was detected in laminae III-X at the lumbar level after reconnection of sectioned DR. This indicated transportation through the peripheral DRG neuron axons. Consistently, a substantial proportion of CTB-positive axons, in deep laminae of the spinal cord, expressed NF200, a marker of large diameter sensory axons.

Moreover, the CTB was also visualized by intravital microscopy and was followed in its pathway from the root, through the DREZ and on to the dorsal horn.

Recording of SEPs showed that electrical stimulation of the peripheral sensory receptors induced signals routed to the spinal cord through the reconstructed sensory pathway. Recovered SEPs were ab-

sent in control animals after DR surgical reconnection, confirming that surgery is not sufficient to reconstruct the sensory pathway. The recovery of sensory perception was nonetheless partial, shown by the low amplitude and surface of electrical signals routed in the reconstructed pathway, as compared to intact rats.

These results demonstrate the efficacy of the combined transplant of cells and scaffold: the scaffold was able to maintain the avulsed root in the right position to optimize the reconnection of the two sides and the SDSCs supported the lesioned axons in the regeneration. Axonal regeneration through the peripheral nervous system-CNS interface may also have been facilitated by growth factors spontaneously released by SDSCs. This study confirms the potential of SDSCs in inducing regeneration of dorsal root axons and adds evidence that transplantation of these easily available stem cells could be a candidate for a promising therapeutic approach in recovery from CNS injury

It remains to be determined to what extent partial restoration of sensory perception could be further improved. The combination of partial sensory and motor restoration might result in valuable improvement of arm movement control and would enhance the efficacy of physio-therapeutic treatment.

#### STATEMENT OF INTERESTS

The Authors declare that they have no conflict of interests.

This study was funded in part by Associazione Amici Centro Dino Ferrari and the Italian Ministry of Health (GR-2008-1146615).

#### REFERENCES

1. Martinoli C, Gandolfo N, Perez MM, et al. Brachial plexus and nerves about the shoulder. *Semin Musculoskelet Radiol* 2010; 14(5): 523-546.
2. Tang XQ, Cai J, Nelson KD, et al. Functional repair after dorsal root rhizotomy using nerve conduits and neurotrophic molecules. *Eur J Neurosci* 2004; 20(5): 1211-1218.
3. Carlstedt T. Nerve fibre regeneration across the peripheral-central transitional zone. *J Anat* 1997; 190 (Pt 1): 51-56.
4. Chong MS, Woolf CJ, Haque NS, Anderson PN. Axonal regeneration from injured dorsal roots into the spinal cord of adult rats. *J Comp Neurol* 1999; 410(1): 42-54.
5. Bradbury EJ, Moon LD, Popat RJ, et al. Chondroitinase ABC promotes functional recovery after spinal cord injury. *Nature* 2002; 416(6881): 636-640.
6. Brosamle C, Huber AB, Fiedler M, et al. Regeneration of lesioned corticospinal tract fibers in the adult rat induced by a recombinant, humanized IN-1 antibody fragment. *J Neurosci* 2000; 20(21): 8061-8068.

7. Fawcett JW, Asher RA. The glial scar and central nervous system repair. *Brain Res Bull* 1999; 49(6): 377-391.
8. Li S, Strittmatter SM. Delayed systemic Nogo-66 receptor antagonist promotes recovery from spinal cord injury. *J Neurosci* 2003; 23(10): 4219-4227.
9. Merkler D, Metz GA, Raineteau O, et al. Locomotor recovery in spinal cord-injured rats treated with an antibody neutralizing the myelin-associated neurite growth inhibitor Nogo-A. *J Neurosci* 2001; 21(10): 3665-3673.
10. Silver J, Miller JH. Regeneration beyond the glial scar. *Nat Rev Neurosci* 2004; 5(2): 146-156.
11. Blesch A, Tuszynski MH. Cellular GDNF delivery promotes growth of motor and dorsal column sensory axons after partial and complete spinal cord transections and induces remyelination. *J Comp Neurol* 2003; 467(3): 403-417.
12. Kobayashi NR, Fan DP, Giehl KM, et al. BDNF and NT-4/5 prevent atrophy of rat rubrospinal neurons after cervical axotomy, stimulate GAP-43 and Talphal-tubulin mRNA expression, and promote axonal regeneration. *J Neurosci* 1997; 17(24): 9583-9595.
13. Moccetti I, Wrathall JR. Neurotrophic factors in central nervous system trauma. *J Neurotrauma* 1995; 12(5): 853-870.
14. Novikova LN, Novikov LN, Kellerth JO. Differential effects of neurotrophins on neuronal survival and axonal regeneration after spinal cord injury in adult rats. *J Comp Neurol* 2002; 452(3): 255-263.
15. Schnell L, Schneider R, Kolbeck R, et al. Neurotrophin-3 enhances sprouting of corticospinal tract during development and after adult spinal cord lesion. *Nature* 1994; 367(6459): 170-173.
16. Woerly S, Doan VD, Sosa N, et al. Prevention of gliotic scar formation by NeuroGel allows partial endogenous repair of transected cat spinal cord. *J Neurosci Res* 2004; 75(2): 262-272.
17. Ye JH, Houle JD. Treatment of the chronically injured spinal cord with neurotrophic factors can promote axonal regeneration from supraspinal neurons. *Exp Neurol* 1997; 143(1): 70-81.
18. Ramon-Cueto A, Cordero MI, Santos-Benito FF, Avila J. Functional recovery of paraplegic rats and motor axon regeneration in their spinal cords by olfactory ensheathing glia. *Neuron* 2000; 25(2): 425-435.
19. Ramon-Cueto A, Plant GW, Avila J, Bunge MB. Long-distance axonal regeneration in the transected adult rat spinal cord is promoted by olfactory ensheathing glia transplants. *J Neurosci* 1998; 18(10): 3803-3815.
20. Takami T, Oudega M, Bates ML, et al. Schwann cell but not olfactory ensheathing glia transplants improve hindlimb locomotor performance in the moderately contused adult rat thoracic spinal cord. *J Neurosci* 2002; 22(15): 6670-6681.
21. Xu XM, Chen A, Guenard V, et al. Bridging Schwann cell transplants promote axonal regeneration from both the rostral and caudal stumps of transected adult rat spinal cord. *J Neurocytol* 1997; 26(1): 1-16.
22. Neumann S, Bradke F, Tessier-Lavigne M, Basbaum AI. Regeneration of sensory axons within the injured spinal cord induced by intraganglionic cAMP elevation. *Neuron* 2002; 34(6): 885-893.
23. Qiu J, Cai D, Dai H, et al. Spinal axon regeneration induced by elevation of cyclic AMP. *Neuron* 2002; 34(6): 895-903.
24. Dergham P, Ellezam B, Essagian C, et al. Rho signaling pathway targeted to promote spinal cord repair. *J Neurosci* 2002; 22(15): 6570-6577.
25. Fouad FS, Wright JM, Plourde G 2<sup>nd</sup>, et al. Synthesis and protein degradation capacity of photoactivated enediynes. *J Org Chem* 2005; 70(24): 9789-97.
26. Fournier AE, Takizawa BT, Strittmatter SM. Rho kinase inhibition enhances axonal regeneration in the injured CNS. *J Neurosci* 2003; 23(4): 1416-1423.
27. Cummings BJ, Uchida N, Tamaki SJ, et al. Human neural stem cells differentiate and promote locomotor recovery in spinal cord-injured mice. *Proc Natl Acad Sci U S A* 2005; 102(39): 14069-14074.
28. Heine W, Conant K, Griffin JW, Hoke A. Transplanted neural stem cells promote axonal regeneration through chronically denervated peripheral nerves. *Exp Neurol* 2004; 189(2): 231-240.
29. Murakami T, Fujimoto Y, Yasunaga Y, et al. Transplanted neuronal progenitor cells in a peripheral nerve gap promote nerve repair. *Brain Res* 2003; 974(1-2): 17-24.
30. Marchesi C, Pluderi M, Colleoni F, et al. Skin-derived stem cells transplanted into resorbable guides provide functional nerve regeneration after sciatic nerve resection. *Glia* 2007; 55(4): 425-438.
31. Dezawa M, Takahashi I, Esaki M, et al. Sciatic nerve regeneration in rats induced by transplantation of in vitro differentiated bone-marrow stromal cells. *Eur J Neurosci* 2001; 14(11): 1771-1776.
32. Hou SY, Zhang HY, Quan DP, et al. Tissue-engineered peripheral nerve grafting by differentiated bone marrow stromal cells. *Neuroscience* 2006; 140(1): 101-110.
33. Keilhoff G, Goehl A, Langnese K, et al. Transdifferentiation of mesenchymal stem cells into Schwann cell-like myelinating cells. *Eur J Cell Biol* 2006; 85(1): 11-24.
34. Mimura T, Dezawa M, Kanno H, et al. Peripheral nerve regeneration by transplantation of bone marrow stromal cell-derived Schwann cells in adult rats. *J Neurosurg* 2004; 101(5): 806-812.
35. Tohill M, Mantovani C, Wiberg M, Terenghi G. Rat bone marrow mesenchymal stem cells express glial markers and stimulate nerve regeneration. *Neurosci Lett* 2004; 362(3): 200-203.
36. Belicchi M, Pisati F, Lopa R, et al. Human skin-derived stem cells migrate throughout forebrain and differentiate into astrocytes after injection into adult mouse brain. *J Neurosci Res* 2004; 77(4): 475-486.
37. Gorio A, Torrente Y, Madaschi L, et al. Fate of autologous dermal stem cells transplanted into the spinal cord after traumatic injury (TSCI). *Neuroscience* 2004; 125(1): 179-189.
38. Laemmel E, Genet M, Le Goualher G, et al. Fibered confocal fluorescence microscopy (Cell-viZio) facilitates extended imaging in the field of microcirculation. A comparison with intravital microscopy. *J Vasc Res* 2004; 41(5): 400-411.
39. Bottai D, Cigognini D, Madaschi L, et al. Embryonic stem cells promote motor recovery and affect inflammatory cell infiltration in spinal cord injured mice. *Exp Neurol* 2010; 223(2): 452-463.
40. Kumagai G, Okada Y, Yamane J, et al. Roles of ES cell-derived gliogenic neural stem/progenitor cells in functional recovery after spinal cord injury. *PLoS One* 2009; 4(11): e7706.

41. Tsuji O, Miura K, Fujiyoshi K, et al. Cell therapy for spinal cord injury by neural stem/progenitor cells derived from iPS/ES cells. *Neurotherapeutics* 2011; 8(4): 668-676.
42. Cao QL, Zhang YP, Howard RM, et al. Pluripotent stem cells engrafted into the normal or lesioned adult rat spinal cord are restricted to a glial lineage. *Exp Neurol* 2001; 167(1): 48-58.
43. Webber DJ, Bradbury EJ, McMahon SB, Minger SL. Transplanted neural progenitor cells survive and differentiate but achieve limited functional recovery in the lesioned adult rat spinal cord. *Regen Med* 2007; 2(6): 929-945.
44. Lipson AC, Widenfalk J, Lindqvist E, et al. Neurotrophic properties of olfactory ensheathing glia. *Exp Neurol* 2003; 180(2): 167-171.
45. Ziegler MD, Hsu D, Takeoka A, et al. Further evidence of olfactory ensheathing glia facilitating axonal regeneration after a complete spinal cord transection. *Exp Neurol* 2011; 229(1): 109-119.
46. Agudo M, Woodhoo A, Webber D, et al. Schwann cell precursors transplanted into the injured spinal cord multiply, integrate and are permissive for axon growth. *Glia* 2008; 56(12): 1263-1270.
47. Boido M, Garbossa D, Fontanella M, Ducati A, Vercelli A. Mesenchymal Stem Cell Transplantation Reduces Glial Cyst and Improves Functional Outcome After Spinal Cord Compression. *World Neurosurg* 2012; 81(1): 183-190.
48. Gu W, Zhang F, Xue Q, et al. Transplantation of bone marrow mesenchymal stem cells reduces lesion volume and induces axonal regrowth of injured spinal cord. *Neuropathology* 2010; 30(3): 205-217.
49. Mothe AJ, Bozkurt G, Catapano J, et al. Intrathecal transplantation of stem cells by lumbar puncture for thoracic spinal cord injury in the rat. *Spinal Cord* 2011; 49(9): 967-973.
50. Hu SL, Luo HS, Li JT, et al. Functional recovery in acute traumatic spinal cord injury after transplantation of human umbilical cord mesenchymal stem cells. *Crit Care Med* 2010; 38(11): 2181-2189.
51. Nakajima H, Uchida K, Guerrero AR, et al. Transplantation of mesenchymal stem cells promotes an alternative pathway of macrophage activation and functional recovery after spinal cord injury. *J Neurotrauma* 2012; 29(8): 1614-1625.
52. Fernandes KJ, McKenzie IA, Mill P, et al. A dermal niche for multipotent adult skin-derived precursor cells. *Nat Cell Biol* 2004; 6(11): 1082-1093.
53. Toma JG, Akhavan M, Fernandes KJ, et al. Isolation of multipotent adult stem cells from the dermis of mammalian skin. *Nat Cell Biol* 2001; 3(9): 778-784.
54. Grimoldi N, Colleoni F, Tiberio F, et al. Stem Cell Salvage of injured peripheral nerve. *Cell Transplant* 2013; 24(2): 213-222.
55. Gomez VM, Averill S, King V, et al. Transplantation of olfactory ensheathing cells fails to promote significant axonal regeneration from dorsal roots into the rat cervical cord. *J Neurocytol* 2003; 32(1): 53-70.
56. Li Y, Carlstedt T, Berthold CH, Raisman G. Interaction of transplanted olfactory-ensheathing cells and host astrocytic processes provides a bridge for axons to regenerate across the dorsal root entry zone. *Exp Neurol* 2004; 188(2): 300-308.